Available online at www.sciencedirect.com

SCIENCE DIRECT®

International Journal of Multiphase Flow 31 (2005) 757–766

International Journal of Multiphase Flow

www.elsevier.com/locate/ijmulflow

Brief communication

Two-phase flow regime maps for air-lift pump vertical upward gas–liquid flow

V.C. Samaras, D.P. Margaris *

Fluid Mechanics Lab., Mechanical Engineering and Aeronautics Dept., University of Patras, GR-26500 Patras, Greece

Received 7 June 2004; received in revised form 24 March 2005

1. Introduction

The flow pattern maps available in literature were first developed for the petrochemical industry (Baker, 1954) for flow of oil and gas in large diameter pipes. Subsequently, the adiabatic flow pattern maps were developed as general flow pattern maps (for example, Hewitt and Roberts, 1969; Taitel et al., 1980). In recent years, a number of flow pattern maps have been developed for specific conditions such as small diameter tubes, evaporation or condensation, and compact heat exchanger geometries.

The main task is to group together the basic flow structures and define a few basic patterns. This is by no means well defined and indeed many flow patterns exist as individual researchers group the flow patterns somewhat differently depending on their own interpretations. Basically the attitude of most practitioners is to minimize the number of flow pattern groups and to group together the flow structures that has basically the same character pertaining to the distribution of the interfaces.

When designing devices in which a two-phase flow occurs, the determination of a flow regime is one of the most essential problems. Different flow regimes may arise, which are depending on the flux of both phases, properties of various factors as well as dimensions and location of a channel. The ranges of occurrence of particular two-phase flow regimes are generally presented in diagrams, called flow regime maps, in the form of areas divided by transition lines. In the literature there is a large number of such works which vary considerably and there are only quite a few

* Corresponding author. Tel./fax: +30 2610 997202.
E-mail address: margaris@mech.upatras.gr (D.P. Margaris).
URL: http://fml.mech.upatras.gr (D.P. Margaris).

0301-9322/$ - see front matter
doi:10.1016/j.ijmultiphaseflow.2005.03.001

universal flow regime maps which could be considered correct for the wide area of variables. In the present paper, an attempt has been made to work out a new flow regime map, quite convenient in presenting two-phase airlift pump performance and regime transitions.

2. The new regime map

A very wide variety of flow regimes have been defined in the literature; this results partly from the subjective nature of flow-regime definitions and partly from a variety of names being given to essentially the same regime. Hewitt and Roberts (1969) designate five basic patterns for up flow namely, bubble flow, slug or plug flow, churn flow, annular flow and wispy-annular flow, defined as follows:

1. Bubble flow. The liquid is continuous, and a dispersion of bubbles flows within the liquid continuum.
2. Slug or plug flow. At higher gas flows, bubble coalescence occurs, and eventually the bubble diameter approaches that of the tube. When this occurs, large, characteristically bullet-shaped bubbles are formed.
3. Churn flow. With increasing flow velocity, a breakdown of the slug flow bubbles leads to an unstable flow regime in which there is an oscillatory motion of the liquid upward and downward in the tube.
4. Annular flow. The liquid flows on the wall of the tube as a film, and the gas phase flows in the centre. Usually, some of the liquid phase is entrained as small droplets in the gas core.
5. Wispy annular flow. As the liquid flow rate is increased, the concentration of drops in the gas core increases; ultimately, droplet coalescence in the core leads to large lumps or streaks (wisps) of liquid in the gas core. This regime is characteristic of flows with high mass flux.

Table 1 lists the flow regimes identified in gas–liquid vertical upward flow systems by several authors, according also to Bi and Grace (1996). Table 2 lists the flow regime maps of two-phase flow in vertical pipes with corresponding parameters, according also to Troniewski and Ulbrich (1984).

Table 1
Proposed flow regimes in the two-phase literature

Author	Flow regimes
Gosline (1936)	Bubble Slug Annular Liquid dispersed
Galegar et al. (1954)	Aerated Slug Turbulent Semi-annular Annular
Wallis (1969)	Bubble Slug Annular Drops
Govier and Aziz (1972)	Bubble Slug Froth Annular
Hewitt (1977)	Bubble Slug Churn Wispy-annular Annular
Taitel et al. (1980)	Bubble Slug Churn Annular Mist
Weisman and Kang (1981)	Bubble Plug Churn Annular
Mishima and Ishii (1984)	Bubble Slug Churn Annular
Brauner and Barnea (1986)	Dispersed bubble Slug Churn Annular
Bilicki and Kestin (1987)	Bubbly Slug Froth Annular Mist

Table 2
Proposed flow regime maps with corresponding coordinates

Author	Coordinates	Explanation
Galegar et al. (1954)	$G_{Ls} - G_{Gs}$	G the mass flux (liquid and gas), s for superficial
Kozlov (1954)	$u_T - \varepsilon$	u the linear velocity, ε the void fraction, T for total
Griffith and Wallis (1961)	$Fr_T - \varepsilon$	Fr the Froude number
Quandt (1965)	$x - G_T$	x the gas mass quality
Hewitt and Roberts (1969)	$u_{Ls}^2\rho_L - u_{Gs}^2\rho_G$	ρ the density, G for gas, L for liquid
Wallis (1969)	$u_{Ls} - u_{Gs}$	
Hobler and Kedzierski (1970)	$\frac{u_{Gs}}{u_{Ls}} - u_{Ls}$	
Brauner and Barnea (1986)	$u_{Ls} - u_{Gs}$	

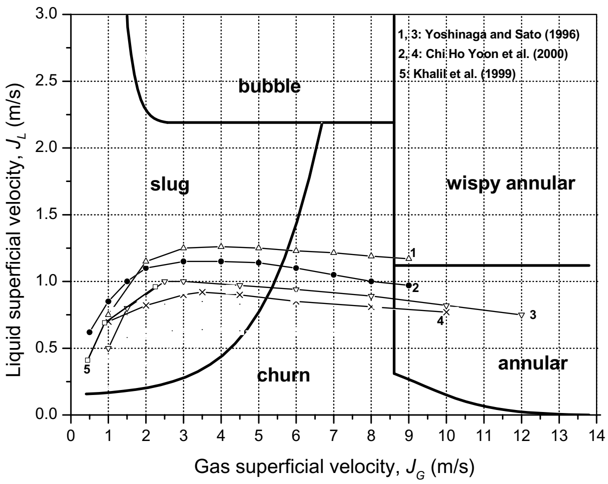

Fig. 1. Presentation of air-lift pump performance on the new regime map.

The aim of the present analysis is the transformation of flow regime maps, given in the literature, into a selected coordinate system. Although parameters including the physical properties of phases could give the best possibility for working out universal flow regime maps, phase velocities and fluxes are undoubtedly the most convenient when used. That is why these parameters were chosen for presentation of the new flow regime map. Fig. 1 shows this new regime map, received merely from Hewitt and Roberts (1969) by linearising and changing coordinates and parameters. In the present map superficial velocities J_G and J_L correspond to u_{Gs} and u_{Ls} of the original map. The main concept for the transformation of the flow regime map is that the characteristic curve of an air-lift pump is given as a function of $J_L(J_G)$. This is not a new map, but a very simple to be used, showing directly the measured data and the flow regime transitions.

3. Air-lift pump performance presented on the new regime map

The air-lift pump, which was originally thought to be applicable for a few simple uses like pumping water, has been utilized as a means of conveying slurries in mining and transporting explosive/poisonous liquid. More recently, it has been reported by Kamata and Ito (1995) that in the steel making process, although the principle of the air-lift pump is applied only to an RH vacuum degasser to circulate molten steel and to remove hydrogen gas, carbon and unmetallic inclusions in molten steel, the simplicity of the equipment may make it applicable for the transportation of molten iron/steel between different refining processes.

It seems to be very difficult to establish an economically optimum condition for operation performance of air-lift pump, since the theoretical model to predict the flow characteristics in full detail has not exactly built yet. It may be commonly accepted that one of the main factors which make it extremely difficult is the transitions of the flow pattern of gas-phase. When gas–liquid mixtures flow upward in a vertical pipe, the two phases distribute in a number of patterns, each characterizing the radical and/or axial distribution of liquid and gas.

Several experimental data from air-lift pump performance are shown in Fig. 1. Curves 1 and 3, derived from Yoshinaga and Sato (1996), represent the performance of an air-lift pump with 6.74 m length upriser and tube diameter of 40 mm and 26 mm respectively. Curves 2 and 4, derived from Yoon et al. (2000), represent the performance of an air-lift pump with 3.64 m length upriser and tube diameter of 30 mm and 20 mm respectively. Finally, curve 5, derived from Khalil et al. (1999), represents the performance of an air-lift pump with 2 m length upriser and tube diameter of 25.4 mm. For all the above installations the submergence ratio was 0.8.

4. Void fraction regime map

Another important issue is to construct a map of void fraction versus gas superficial velocity to display flow regimes.

According to Wallis (1969), the void fraction for slug and churn regimes can be calculated by

$$\varepsilon_G = \frac{J_G}{1.2(J_G + J_L) + 0.345\sqrt{gD(\rho_L - \rho_G)/\rho_L}}, \tag{1}$$

where D, diameter of pipe, and g, gravitational acceleration.

The transition lines from bubble to slug, slug to churn and churn to annular, shown in Fig. 1, are given by the following equations respectively:

$$J_L = 2.17 + 35.45\,e^{-\frac{J_G}{0.40}}, \tag{2}$$

$$J_L = 0.047\,e^{\frac{J_G}{1.75295}}, \tag{3}$$

$$J_L = 0.1385 + 2.085 \times 10^{47}\,e^{-\frac{J_G}{0.07853}}. \tag{4}$$

Substituting these equations into Eq. (1) we get the following expressions of void fraction ε_G versus gas superficial velocity J_G, giving the corresponding transition lines in a void fraction regime map, shown in Fig. 2:

$$\varepsilon_G = \frac{J_G}{1.2\left(J_G + 2.17 + 35.45\,e^{-\frac{J_G}{0.4}}\right) + 0.345\sqrt{gD(\rho_L - \rho_G)/\rho_L}}, \tag{5}$$

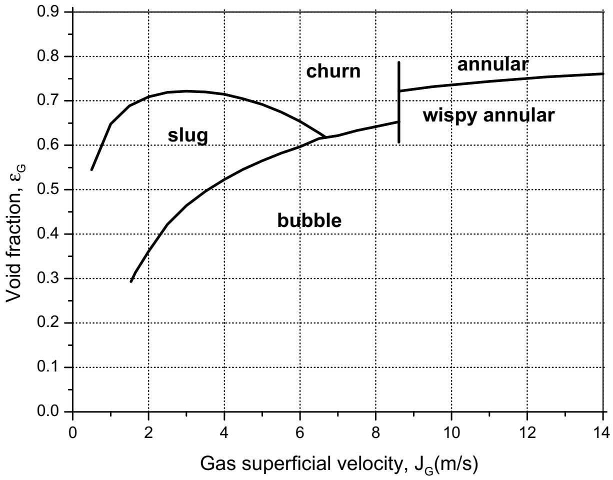

Fig. 2. Two-phase flow regime map of void fraction ε_G versus gas superficial velocity J_G.

$$\varepsilon_G = \frac{J_G}{1.2\left(J_G + 0.047\,e^{\frac{J_G}{1.75295}}\right) + 0.345\sqrt{gD(\rho_L - \rho_G)/\rho_L}}, \tag{6}$$

$$\varepsilon_G = \frac{J_G}{1.2\left(J_G + 0.1385 + 2.085 \times 10^{47}\,e^{-\frac{J_G}{0.07853}}\right) + 0.345\sqrt{gD(\rho_L - \rho_G)/\rho_L}}. \tag{7}$$

For annular flow regime Eq. (1) is not valid. So another procedure is used. A correlation for void fraction in upwards annular flow, given by Wallis (1969), is

$$\frac{J_G^*}{1 - 2.85(1 - \varepsilon_G)} - \frac{J_L^*}{2.85(1 - \varepsilon_G)} = 0.775, \tag{8}$$

where

$$J_G^* = \frac{J_G \rho_G^{1/2}}{\{gD(\rho_L - \rho_G)\}^{1/2}} \tag{9}$$

and

$$J_L^* = \frac{J_L \rho_L^{1/2}}{\{gD(\rho_L - \rho_G)\}^{1/2}}. \tag{10}$$

Introducing Eqs. (9) and (10) into Eq. (8) and rearranging to account for $(1 - \varepsilon_G)$, the void fraction in this regime can be calculated by

$$A(1 - \varepsilon_G)^2 + B(1 - \varepsilon_G) + C = 0, \tag{11}$$

where

$$A = 6.295\{gD(\rho_L - \rho_G)\}^{1/2},$$
$$B = 2.85\left\{J_G\rho_G^{1/2} + J_L\rho_L^{1/2} - 0.775\{gD(\rho_L - \rho_G)\}^{1/2}\right\}, \quad (12)$$
$$C = -J_L\rho_L^{1/2},$$

and the only acceptable solution (since $\varepsilon_G > 1$ has no meaning) is

$$\varepsilon_G = 1 - \left(\frac{-B + (B^2 - 4AC)^{1/2}}{2A}\right). \quad (13)$$

In order to express ε_G as a function of J_G from Fig. 1, for the annular flow regime, we get

$$J_L = 1.12\ \text{m/s}, \quad (14)$$

which by substitution into Eq. (13) gives an $\varepsilon_G = f(J_G)$ function. This expression represents the transition line between annular and wispy annular, shown in Fig. 2.

5. Experimental apparatus and procedure

Experimental data of the Fluid Mechanics Laboratory of the Patras University are included below. The installation (Fig. 3, Table 3) contains two sizes of upriser tube (28 mm and 40 mm),

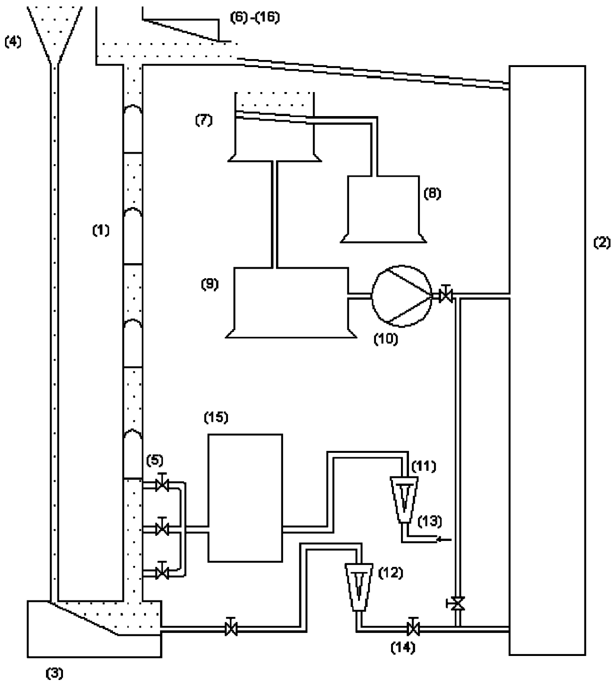

Fig. 3. Air-lift pump laboratory scale installation.

Table 3
Air-lift pump laboratory scale installation parts list

1	Upriser (40 mm and 28 mm)
2	Main water tank (400 mm)
3	Suction box
4	Solid particles box
5	Air injection points
6	Air–water–solids separator (3-phase)
7	Water–solids separator
8	Solid particles scale
9	Auxiliary water tank (250 l)
10	Pump
11	Air rotameters (2 sizes)
12	Water rotameters (2 sizes)
13	Air compressor
14	Water valves
15	Control panel
16	Air–water separator (2-phase)

the possibility of two and three phase flow experiments (with several particle diameters and densities), the extra possibility of forced flow via auxiliary pump (in order to realize bubble flow regime, impossible for small diameter airlift pump performance) and a frequency inverter monitored pump in order to stabilize the submergence ratio during experiments. The air is injected in three different levels, thus achieving several combinations of submergence ratios.

At low gas flow rate the flow is unstable. Visual observation reveals regular oscillations, with the gas entering periodically the liquid pipe (flow reversal). The flow at the riser outlet is strongly pulsating. When the gas flow rate is increased, the strength of the oscillations decreases. For the operating points used in this paper the flow oscillations are still apparent, but there is no more reverse flow. However, the gas–liquid interface, downstream of the injection tee, fluctuates regularly. Further increasing the gas flow rate the flow stabilizes. There are sudden, very strong oscillations, which is the case where the liquid enters periodically the gas pipe.

The assumptions of ideal gas, adiabatic flow, homogeneous pressure and temperature in the gas pipe are made. The gas slip velocity, the gas velocity and the void fraction are expressed using the steady-state relationships.

Several curves are shown in Fig. 4. It represents the validation of diagram in Fig. 1 with experimental data. Experimental data are presented from the small diameter air-lift pump lab scale installation of the laboratory. The values covered are for the gas superficial velocity from 1 m/s to 10 m/s and for the liquid superficial velocity from 0.5 m/s to 2.75 m/s. Three of them represent the performance of a 40 mm air-lift pump upriser, for several submergence ratios, 0.8, 0.7 and 0.6. Four different flow regimes are indicated, slug, churn, annular and wispy annular. Obviously the liquid volumetric flux is greater for submergence ratio 0.8 than those for 0.7 and 0.6, for the same gas volumetric flux. A value of liquid superficial velocity of 1.5 m/s is the maximum value achieved for this 40 mm upriser tube, for a submergence ratio of 0.8. A fourth curve, the lowest one in Fig. 4, represents the performance of a 28 mm air-lift pump upriser, for the submergence ratio of 0.6. It was selected because it represents the minimum value of liquid superficial velocity achieved for this 28 mm upriser tube. There are also curves, for the same 28 mm upriser for

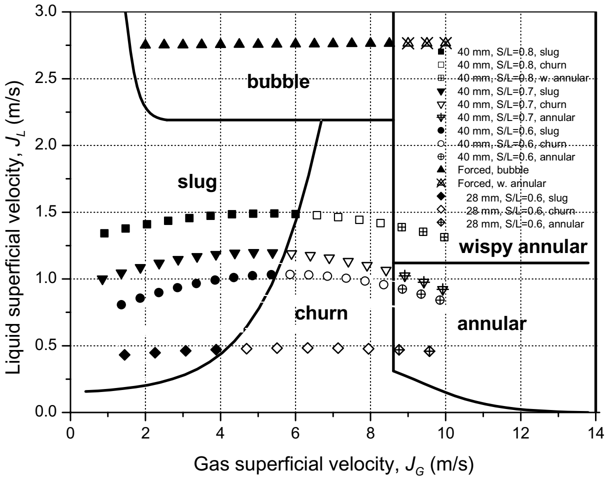

Fig. 4. Validation of diagram in Fig. 1 with experimental data.

submergence ratios of 0.8 and 0.7, available in the laboratory. Finally a fifth curve, the upper one in Fig. 4, is shown, achieved via an auxiliary pump (not from simple air-lift pump operation) in order to operate in bubble and wispy annular flow regime. Every point of these five curves is quite identified. Several different symbols were used in order to determine the transition areas for different flow regimes.

By using Eq. (1) for the slug and churn flow regimes, Eqs. (12)–(14) for the annular and wispy annular flow regimes and the following Eq. (15), according to Wallis (1969), for the bubble flow regime, it is possible to represent the above mentioned five experimental curves on the $\varepsilon_G = f(J_G)$ map (Fig. 5):

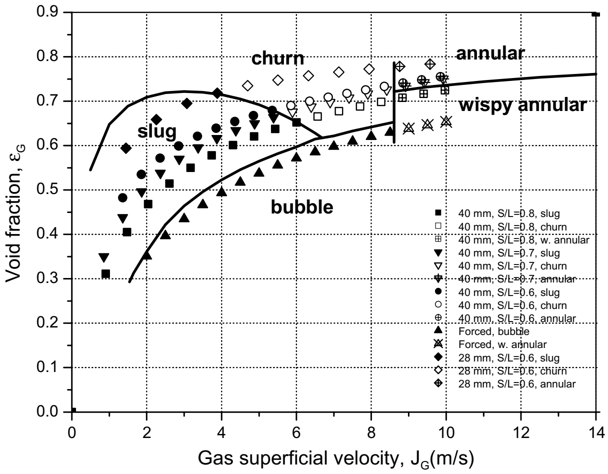

Fig. 5. Validation of diagram in Fig. 2 with experimental data.

$$\varepsilon_{\mathrm{G}} = \frac{J_{\mathrm{G}}}{1.2(J_{\mathrm{G}} + J_{\mathrm{L}})}. \tag{15}$$

Fig. 5 represents the validation of diagram in Fig. 2 with experimental data.

6. Discussion

Two new regime maps are introduced in the present paper. The first one is substantially the well-known Hewitt and Roberts (1969) regime map, transformed and suitable for representing the flow performance of an air-lift pump. In order to achieve this, the gas superficial velocity J_{G} and the liquid superficial velocity J_{L} are used as coordinates of the map. The researchers of this scientific area use mainly these coordinates for the representation of an air-lift pump performance. The advantage of such a presentation of these data in the transformed regime map is the direct view of the flow behaviour inside the air-lift pump, concerning the regime transitions.

A second map is derived from this map, giving the void fraction ε_{G} versus gas superficial velocity J_{G}. By substituting the functions $J_{\mathrm{L}} = f(J_{\mathrm{G}})$ from Fig. 1 into equations $\varepsilon_{\mathrm{G}} = f(J_{\mathrm{G}}, J_{\mathrm{L}})$, the equations derived represent the transition lines as functions $\varepsilon_{\mathrm{G}} = f(J_{\mathrm{G}})$. It is also possible to represent the air-lift pump performance (characteristic line) in this second map. The advantage of this map is that, having as experimental data only the gas superficial velocity (air injected inside the upriser) and the visual designation of the flow regime, it is possible to estimate the void fraction range of values. As an example, for slug regime (visual observation) and gas superficial velocity $J_{\mathrm{G}} = 5$ m/s we get from Fig. 2. $\varepsilon_{\mathrm{G}} = 0.57$–$0.68$, for annular regime and gas superficial velocity $J_{\mathrm{G}} = 9$ m/s we get $\varepsilon_{\mathrm{G}} \geqslant 0.73$.

Five experimental curves were shown on these two regime maps, containing 82 quite identified experimental points of the performance of the small diameter air-lift pump lab scale installation of the laboratory. The regime transitions areas were totally validated through these experimental data.

As a final conclusion, these proposed maps constitute useful tools for the presentation of the performance of an air-lift pump, the direct view of the regime transitions and the estimation of the void fraction.

References

Baker, O., 1954. Simultaneous flow of oil and gas. Oil Gas J. 53, 185.

Bi, H.T., Grace, J.R., 1996. Regime transitions: analogy between gas–liquid co-current upward flow and gas–solids upward transport. Int. J. Multiphase Flow 22 (Suppl.), 1–19.

Bilicki, Z., Kestin, J., 1987. Transition criteria for two-phase flow patterns in vertical upward flow. Int. J. Multiphase Flow 13, 283–294.

Brauner, N., Barnea, D., 1986. Slug/churn transition in upward gas–liquid flow. Chem. Eng. Sci. 41, 159–163.

Galegar, W.C., Stovall, W.B., Huntington, R.L., 1954. More data on two-phase vertical flow. Petrol. Refiner 33, 208.

Gosline, J.E., 1936. Experiments on the vertical flow of gas–liquid mixtures in glass pipes. Trans. Am. Inst. Mining, Meter. Petrol. Eng. 118, 56–70.

Govier, G.W., Aziz, K., 1972. The Flow of Complex Mixtures in Pipes. Van Nostrand-Reinhold, New York.

Griffith, P., Wallis, G.B., 1961. Two-phase slug flow. Trans. ASME, J. Heat Transfer 83C, 307.

Hewitt, G.F., 1977. Flow patterns. In: Two-phase Flow and Heat Transfer. Oxford University Press, pp. 18–39 (Chapter 2).
Hewitt, G.F., Roberts, D.N., 1969. Studies of two-phase flow patterns by simultaneous X-ray and flash photography. UKAEA Report AERE-M2159.
Hobler, T., Kedzierski, S., 1970. Hydrodynamics of rivulet flow on a vertical surface. Chem. Stos. 7, 157.
Kamata, C., Ito, K., 1995. Cold model experiments on the application of gas lift pump to the transportation of molten metal. ISIJ Int. 35, 859–865.
Khalil, M.F., Elshorbagy, K.A., Kassab, S.Z., Fahmy, R.I., 1999. Effect of air injection method on the performance of an air lift pump. Int. J. Heat Fluid Flow 20, 598–604.
Kozlov, B.K., 1954. Forms of flow of gas–liquid mixtures and their stability limits in vertical tubes. Z. Technic. Fiz. 12, 2285.
Mishima, K., Ishii, M., 1984. Flow regime transition criteria for upward two-phase flow in vertical tubes. Int. J. Heat Mass Transfer 27, 723–737.
Quandt, E.R., 1965. Semiparametric estimation of heteroscedastic binary choice sample selection models under symmetry. Chem. Eng. Prog. Symp. 61, 128.
Taitel, Y., Barnea, D., Dukler, A.E., 1980. Modeling flow pattern transitions for steady upward gas–liquid flow in vertical tubes. AIChE J. 26, 345–354.
Troniewski, L., Ulbrich, R., 1984. The analysis of flow regime maps of two-phase gas–liquid flow in pipes. Chem. Eng. Sci. 39, 1213–1224.
Wallis, G.B., 1969. One-dimensional Two-phase Flow. McGraw-Hill, New York.
Weisman, J., Kang, S.Y., 1981. Flow pattern transitions in vertical and upwardly inclined lines. Int. J. Multiphase Flow 7, 271–291.
Yoon, C.H., Kwon, K.S., Kwon, O.K., Kwon, S.K., Kim, K., Lee, D.K., 2000. An experimental study on lab scale air-lift pump flowing solid–liquid–air three-phase mixture. In: Proc. International Offshore and Polar Conference, Seattle, USA. pp. 515–521.
Yoshinaga, T., Sato, Y., 1996. Performance of an air-lift pump for conveying coarse particles. Int. J. Multiphase Flow 22, 223–238.